

# Asymmetries in $\bar{B}_d^0 \rightarrow \bar{K}^{*0} e^+ e^-$ decay and contribution of vector resonances

Alexander Yu. Korchin<sup>1,\*</sup> and Vladimir A. Kovalchuk<sup>1,†</sup>

<sup>1</sup>*NSC ‘Kharkov Institute of Physics and Technology’, 61108 Kharkov, Ukraine*

(Dated: today)

The fully differential angular distribution for the rare flavor-changing neutral current decay  $\bar{B}_d^0 \rightarrow \bar{K}^{*0} (\rightarrow K^- \pi^+) e^+ e^-$  is studied. The emphasis is placed on accurate treatment of the contribution from the processes  $\bar{B}_d^0 \rightarrow \bar{K}^{*0} (\rightarrow K^- \pi^+) V$  with intermediate vector resonances  $V = \rho(770), \omega(782), \phi(1020), J/\psi, \psi(2S), \dots$  decaying into the  $e^+ e^-$  pair. The two versions of the vector-meson-dominance model for the transition  $V \gamma$  are used and tested. The present method of including vector resonances is also compared with the existing in the literature method. The electron-positron invariant mass dependence of the branching ratio and various asymmetries is calculated. The branching ratio, longitudinal polarization fraction of the  $\bar{K}^{*0}$  meson, transverse asymmetry  $A_T^{(2)}$  and forward-backward asymmetry are compared with data from Belle and CDF, and predictions for experiments at LHCb are made.

PACS numbers: 13.20.He, 13.25.Hw, 12.40.Vv

## I. INTRODUCTION

The investigation of rare  $B$  decays induced by the flavor-changing neutral current (FCNC) transitions  $b \rightarrow s$  and  $b \rightarrow d$  represents an important test of the standard model (SM) and its extensions (see [1] for a review).

Among the rare decays, the process  $b \rightarrow s \ell^+ \ell^-$ , where the virtual photon is converted to the lepton pair, is of considerable interest. This decay proceeds through a loop (penguin) diagram, to which high-mass particles introduced in various extensions to the SM may contribute with sizable amplitudes. In this decay the angular distributions and lepton polarizations can probe the chiral structure of the matrix element [2–8] and thereby effects of the new physics (NP) beyond the SM.

In order to unambiguously measure effects of NP in the observed process  $\bar{B}_d^0 \rightarrow \bar{K}^{*0} (\rightarrow K^- \pi^+) \ell^+ \ell^-$  ( $\ell = e, \mu$ ), mediated by  $b \rightarrow s \ell^+ \ell^-$  decay, one needs to calculate the SM predictions with a high accuracy. The amplitude in the SM consists of the short-distance (SD) and long-distance (LD) contributions. The former are expressed in terms of the Wilson coefficients  $C_i$  calculated in perturbative QCD up to a certain order in  $\alpha_s(\mu)$ ; they carry information on processes at energy scales  $\sim m_W, m_t$ . The LD effects describing the hadronization process are expressed in terms of matrix elements of several  $b \rightarrow s$  operators between the initial  $B$  and the  $K^*$  final state. These hadronic matrix elements are parameterized in terms of form factors [4] that are calculated in various approaches (see, e.g., [9, 10]).

The additional LD effects, originating from intermediate vector resonances  $\rho(770), \omega(782), \phi(1020), J/\psi(1S), \psi(2S), \dots$ , in general, may complicate theoretical interpretation and make it more model dependent. The vector resonances modify the amplitude and thus may induce,

for example, the right-handed currents which are absent in the SM.

Present experimental studies [11–13] of the  $B \rightarrow K^* \ell^+ \ell^-$  decay aim at the search of effects of the NP in the whole region of dilepton invariant mass  $m_{ee} \equiv \sqrt{q^2}$  GeV (here  $q = q_+ + q_-$ ). In these analyses certain cuts are applied in order to exclude a rather big charmonia contribution.

Recently also the region of small dilepton invariant mass,  $m_{ee} \lesssim 1$  GeV, attracted attention [2], as having a potential for searching signatures of the NP. The authors of [14] analyzed the azimuthal angular distribution in the decay  $\bar{B}^0 \rightarrow \bar{K}^{*0} \ell^+ \ell^-$  in this region, to test the possibility to measure this distribution at the LHCb. They have shown the feasibility of measurements with small systematic uncertainties. In Ref. [15] the influence of the low-lying resonances  $\rho(770), \omega(782)$  and  $\phi(1020)$  on differential branching ratio, polarization fraction of the  $K^{*0}$  and transverse asymmetry  $A_T^{(2)}$  has been studied.

In the present paper we extend calculations of [15] to the whole region of dilepton invariant mass up to  $m_{ee}^{max} = m_B - m_{K^*} = 4.39$  GeV. The effective SM Hamiltonian with the Wilson coefficients in the next-to-next-to-leading order (NNLO) approximation is applied. The LD effects mediated by the resonances, *i.e.*  $\bar{B}^0 \rightarrow \bar{K}^{*0} V \rightarrow \bar{K}^{*0} e^+ e^-$  with  $V = \rho(770), \omega(782), \phi(1020), J/\psi, \psi(2S), \dots$ , are included explicitly in terms of the helicity amplitudes of the decays  $\bar{B}^0 \rightarrow \bar{K}^{*0} V$ . The information on the latter is taken from experiments if available; otherwise it is taken from theoretical predictions.

The fully differential angular distribution over the three angles and dilepton invariant mass for the four-body decay  $\bar{B}_d^0 \rightarrow K^- \pi^+ e^+ e^-$  is analyzed. We define a convenient set of asymmetries which allows one to extract these asymmetries from the angular distribution once sufficient statistics is accumulated. These asymmetries may have sensitivity to various effects of the NP, although in order to see signatures of these effects, the resonance

\*Electronic address: korchin@kipt.kharkov.ua

†Electronic address: koval@kipt.kharkov.ua

contribution should be accurately evaluated.

One of the ingredients in calculation of the resonance contribution is the transition vertex  $V\gamma$ . This vertex is conventionally treated in the vector-meson-dominance (VMD) model. In the present paper we apply two versions of the VMD model (called subsequently VMD1 and VMD2) which result in rather different  $V\gamma$  vertices, in particular, far from the vector-meson mass shell  $q^2 = m_V^2$ . Specifically, due to explicit gauge-invariant construction of the VMD2 Lagrangian the  $V\gamma$  transition is suppressed in the region  $q^2 \ll m_V^2$  (for  $V = J/\psi, \psi(2S), \dots$ ). This observation may be important for estimation of resonance contribution to those asymmetries, which are small in the SM.

One should mention that the  $c\bar{c}$  vector resonances  $J/\psi, \psi(2S), \dots$  have been included earlier in Refs. [16] in the analysis of the  $\bar{B}^0 \rightarrow \bar{K}^{*0} \mu^+ \mu^-$  decay. This method of including resonances has been originally suggested in [17]. In order to see sensitivity of observables to the method of including the  $c\bar{c}$  resonances, we perform calculations using the two methods, and compare the results.

Results of the present calculations are compared with the recent data from Belle (KEKB) and CDF (Tevatron) experiments for the differential branching, asymmetry  $A_T^{(2)}$ , longitudinal polarization fraction of  $K^*$  and forward-backward asymmetry.

The paper is organized as follows. In Sec. II A the fully differential angular distribution is discussed. In Section II B one-dimensional distributions and definition of asymmetries are defined. Section II C contains expressions for the transversity amplitudes in framework of the SM. The models of vector-meson dominance and contributions of vector resonances to the amplitudes are discussed in Sec. II D. Results for the dependence of observables on the invariant mass squared are presented in Sec. III A. In Sec. III B we compare two approaches to inclusion of vector resonances in the amplitudes of the  $\bar{B}_d^0 \rightarrow K^- \pi^+ e^+ e^-$  decay. In Sec. IV we draw conclusions. In Appendix A some details of the calculation of the matrix element and the model of the  $B \rightarrow K^*$  transition form factors are described. Appendix B deals

with calculation of the  $\bar{B}^0 \rightarrow \bar{K}^{*0} V$  amplitudes for the off-mass-shell vector meson  $V$ .

## II. ANGULAR DISTRIBUTIONS AND AMPLITUDES FOR THE $\bar{B}_d^0 \rightarrow \bar{K}^{*0} e^+ e^-$ DECAY

### A. Differential decay rate

The decay  $\bar{B}_d^0 \rightarrow \bar{K}^{*0} e^+ e^-$ , with  $\bar{K}^{*0} \rightarrow K^- \pi^+$  on the mass shell [32], is completely described by four independent kinematic variables: the electron-positron pair invariant-mass squared,  $q^2$ , and the three angles  $\theta_l, \theta_K, \phi$ . In the helicity frame (Fig. 1), the angle  $\theta_l$  ( $\theta_K$ ) is defined as the angle between the directions of motion of  $e^+$  ( $K^-$ ) in the  $\gamma^*$  ( $\bar{K}^{*0}$ ) rest frame and the  $\gamma^*$  ( $\bar{K}^{*0}$ ) in the  $\bar{B}_d^0$  rest frame. The azimuthal angle  $\phi$  is defined as

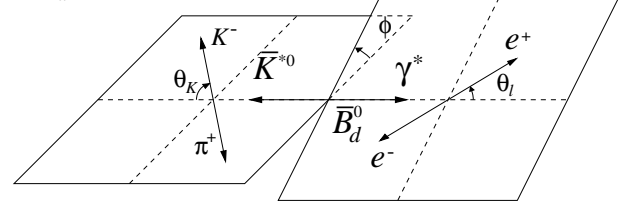


FIG. 1: Definition of helicity angles  $\theta_l, \theta_K$ , and  $\phi$ , for the decay  $\bar{B}_d^0 \rightarrow \bar{K}^{*0} e^+ e^-$ .

the angle between the decay planes of  $\gamma^* \rightarrow e^+ e^-$  and  $\bar{K}^{*0} \rightarrow K^- \pi^+$  in the  $\bar{B}_d^0$  rest frame. The fully differential angular distribution in these coordinates is given by

$$\begin{aligned} \mathcal{W}(\hat{q}^2, \theta_l, \theta_K, \phi) &\equiv \frac{d^4 \Gamma}{d\hat{q}^2 d \cos \theta_l d \cos \theta_K d\phi} / \frac{d\Gamma}{d\hat{q}^2} \\ &= \frac{9}{64\pi} \sum_{k=1}^9 \alpha_k(q^2) g_k(\theta_l, \theta_K, \phi), \quad (1) \end{aligned}$$

where the angular terms  $g_k$  are defined as

$$g_1 = 4 \sin^2 \theta_l \cos^2 \theta_K, \quad g_2 = (1 + \cos^2 \theta_l) \sin^2 \theta_K, \quad g_3 = \sin^2 \theta_l \sin^2 \theta_K \cos 2\phi,$$

$$g_4 = -2 \sin^2 \theta_l \sin^2 \theta_K \sin 2\phi, \quad g_5 = -\sqrt{2} \sin 2\theta_l \sin 2\theta_K \cos \phi, \quad g_6 = -\sqrt{2} \sin 2\theta_l \sin 2\theta_K \sin \phi,$$

$$g_7 = 4 \cos \theta_l \sin^2 \theta_K, \quad g_8 = -2\sqrt{2} \sin \theta_l \sin 2\theta_K \cos \phi, \quad g_9 = -2\sqrt{2} \sin \theta_l \sin 2\theta_K \sin \phi,$$

and the amplitude terms  $\alpha_k$  as

$$\alpha_1 = |a_0|^2 = f_L, \quad \alpha_2 = |a_{\parallel}|^2 + |a_{\perp}|^2 = f_{\parallel} + f_{\perp}, \quad \alpha_3 = |a_{\perp}|^2 - |a_{\parallel}|^2 = f_{\perp} - f_{\parallel}, \quad \alpha_4 = \text{Im}(a_{\parallel} a_{\perp}^*), \quad \alpha_5 = \text{Re}(a_0 a_{\parallel}^*),$$

$$\alpha_6 = \text{Im}(a_0 a_{\perp}^*), \quad \alpha_7 = \text{Re}(a_{\parallel L} a_{\perp L}^* - a_{\parallel R} a_{\perp R}^*), \quad \alpha_8 = \text{Re}(a_{0L} a_{\perp L}^* - a_{0R} a_{\perp R}^*), \quad \alpha_9 = \text{Im}(a_{0L} a_{\parallel L}^* - a_{0R} a_{\parallel R}^*),$$

where  $\hat{q}^2 \equiv q^2/m_B^2$ ,  $m_B$  is the mass of the  $B_d^0$  meson, and

$$\frac{d\Gamma}{d\hat{q}^2} = m_B N^2 \hat{q}^2 \sqrt{\hat{\lambda}} (|A_0|^2 + |A_{\parallel}|^2 + |A_{\perp}|^2). \quad (2)$$

$$a_{iA} a_j^* \equiv a_{iL}(q^2) a_{jL}^*(q^2) + a_{iR}(q^2) a_{jR}^*(q^2), \quad (3)$$

$$a_{iL(R)} \equiv \frac{A_{iL(R)}}{\sqrt{\sum_j |A_j|^2}}. \quad (4)$$

Here  $i, j = (0, \parallel, \perp)$ , we have neglected the electron mass  $m_e$  and  $A_{0L(R)}$ ,  $A_{\parallel L(R)}$  and  $A_{\perp L(R)}$  are the complex decay amplitudes of the three helicity states in the transversity basis,  $f_L$ ,  $f_{\parallel}$  and  $f_{\perp}$  are polarization parameters of the  $K^*$  meson,  $f_L + f_{\parallel} + f_{\perp} = 1$ ,  $\hat{\lambda} \equiv \lambda(1, \hat{q}^2, \hat{m}_{K^*}^2) = (1 - \hat{q}^2)^2 - 2(1 + \hat{q}^2)\hat{m}_{K^*}^2 + \hat{m}_{K^*}^4$ ,  $\hat{m}_{K^*} \equiv m_{K^*}/m_B$ , where  $m_{K^*}$  is the mass of the  $K^{*0}$  meson, and

$$N = |V_{tb}V_{ts}^*| \frac{G_F m_B^2 \alpha_{\text{em}}}{32 \pi^2 \sqrt{3} \pi}.$$

Here,  $V_{ij}$  are the Cabibbo-Kobayashi-Maskawa (CKM) matrix elements [18],  $G_F$  is the Fermi coupling constant,  $\alpha_{\text{em}}$  is the electromagnetic fine-structure constant.

With its rich multidimensional structure, the differential decay rate in Eq. (1) has sensitivity to various effects modifying the SM, such as  $CP$  violation beyond the CKM mechanism and/or right-handed currents. Given sufficient data, all  $\alpha_k$  can, in principle, be completely measured from the full angular distribution in all three angles  $\theta_l$ ,  $\theta_K$ , and  $\phi$ .

### B. One-dimensional angular distributions and asymmetries

The one-dimensional angular distributions in  $\cos \theta_l$  and  $\cos \theta_K$  simply are

$$\begin{aligned} \mathcal{W}_{\theta_l}(\hat{q}^2, \cos \theta_l) &\equiv \frac{d^2 \Gamma}{d\hat{q}^2 d \cos \theta_l} / \frac{d\Gamma}{d\hat{q}^2} = \frac{3}{4} f_L (1 - \cos^2 \theta_l) \\ &+ \frac{3}{8} (1 - f_L) (1 + \cos^2 \theta_l) \\ &+ \frac{d\bar{A}_{\text{FB}}^{(1)}}{d\hat{q}^2} \cos \theta_l \end{aligned} \quad (5)$$

and

$$\begin{aligned} \mathcal{W}_{\theta_K}(\hat{q}^2, \cos \theta_K) &\equiv \frac{d^2 \Gamma}{d\hat{q}^2 d \cos \theta_K} / \frac{d\Gamma}{d\hat{q}^2} = \frac{3}{2} f_L \cos^2 \theta_K \\ &+ \frac{3}{4} (1 - f_L) (1 - \cos^2 \theta_K), \end{aligned} \quad (6)$$

where  $d\bar{A}_{\text{FB}}^{(1)}/d\hat{q}^2$  is the normalized lepton forward-backward asymmetry

$$\begin{aligned} \frac{d\bar{A}_{\text{FB}}^{(1)}}{d\hat{q}^2} &\equiv \int_{-1}^1 \text{sgn}(\cos \theta_l) \mathcal{W}_{\theta_l}(\hat{q}^2, \cos \theta_l) d \cos \theta_l \\ &= \frac{3}{2} \text{Re}(a_{\parallel L} a_{\perp L}^* - a_{\parallel R} a_{\perp R}^*) \equiv A_7. \end{aligned} \quad (7)$$

While  $\mathcal{W}_{\theta_K}(\hat{q}^2, \cos \theta_K)$  depends only on  $f_L$ ,  $\mathcal{W}_{\theta_l}(\hat{q}^2, \cos \theta_l)$  depends both on  $f_L$  and  $d\bar{A}_{\text{FB}}^{(1)}/d\hat{q}^2$ .

The measurement of the lepton forward-backward asymmetry  $d\bar{A}_{\text{FB}}^{(1)}/d\hat{q}^2$  alone is not enough to fully reconstruct the  $\cos \theta_l$  distribution. One can then think about other asymmetries. For any fixed  $z$  in the interval  $[-1, 1]$ , one can define an asymmetry

$$\mathcal{A}_z \equiv \frac{\mathcal{E}_z - \mathcal{P}_z}{\mathcal{E}_z + \mathcal{P}_z}, \quad (8)$$

where

$$\mathcal{E}_z \equiv \int_{-z}^z \mathcal{W}_{\theta}(\hat{q}^2, \cos \theta) d \cos \theta, \quad (9)$$

and

$$\mathcal{P}_z \equiv \left( \int_{-1}^{-z} d \cos \theta + \int_z^1 d \cos \theta \right) \mathcal{W}_{\theta}(\hat{q}^2, \cos \theta). \quad (10)$$

Measuring the asymmetry  $\mathcal{A}_{z_l}$  for  $z = z_l \approx 0.596$  ( $\cos^3 \theta_l + 3 \cos \theta_l - 2 = 0$ ), we can find the fraction of the longitudinal polarization of the  $K^*$  meson

$$\mathcal{A}_{z_l} = 3(2z_l - 1)f_L \approx 0.576f_L, \quad (11)$$

Similarly, measuring the asymmetry  $\mathcal{A}_{z_K}$  for  $z = z_K = 2 \cos \frac{4\pi}{9} \approx 0.347$  ( $\cos^3 \theta_K - 3 \cos \theta_K + 1 = 0$ ), we can find the fraction of the longitudinal polarization of the  $K^*$  meson

$$\mathcal{A}_{z_K} = 3(2z_K - 1)f_L \approx -0.916f_L. \quad (12)$$

Finally, the one-dimensional angular distribution in the angle  $\phi$  between the lepton and meson planes takes the form

$$\begin{aligned} \mathcal{W}_{\phi}(\hat{q}^2, \phi) &\equiv \frac{d^2 \Gamma}{d\hat{q}^2 d\phi} / \frac{d\Gamma}{d\hat{q}^2} = \frac{1}{2\pi} \left( 1 + \frac{1}{2} (1 \right. \\ &\left. - f_L) A_{\text{T}}^{(2)} \cos 2\phi - A_{\text{Im}} \sin 2\phi \right), \end{aligned} \quad (13)$$

$$A_{\text{T}}^{(2)} \equiv \frac{f_{\perp} - f_{\parallel}}{f_{\perp} + f_{\parallel}}, \quad A_{\text{Im}} \equiv \text{Im}(a_{\parallel} a_{\perp}^*), \quad (14)$$

where the asymmetry  $A_{\text{T}}^{(2)}(q^2)$  is sensitive to new physics from right-handed currents, and the amplitude  $A_{\text{Im}}(q^2)$  is sensitive to complex phases in the hadronic matrix elements. Sometimes  $A_{\text{T}}^{(2)}(q^2)$  is called transverse asymmetry [5].

Measurement of the angular distribution in the azimuthal angle  $\phi$  allows one to determine the quantities  $(1 - f_L)A_{\text{T}}^{(2)}$  and  $A_{\text{Im}}$

$$\begin{aligned} A_3 &\equiv \left( \int_0^{\pi/4} d\phi - \int_{\pi/4}^{3\pi/4} d\phi + \int_{3\pi/4}^{5\pi/4} d\phi \right. \\ &\left. - \int_{5\pi/4}^{7\pi/4} d\phi + \int_{7\pi/4}^{2\pi} d\phi \right) \mathcal{W}_{\phi}(\hat{q}^2, \phi) \\ &= \frac{1}{\pi} (1 - f_L) A_{\text{T}}^{(2)} = \frac{f_{\perp} - f_{\parallel}}{\pi}, \end{aligned} \quad (15)$$

$$A_4 \equiv \left( \int_0^{\pi/2} d\phi - \int_{\pi/2}^{\pi} d\phi + \int_{\pi}^{3\pi/2} d\phi - \int_{3\pi/2}^{2\pi} d\phi \right) \mathcal{W}_\phi(\hat{q}^2, \phi) = -\frac{2}{\pi} A_{\text{Im}}. \quad (16)$$

Measurement of the azimuthal angle dependence of the forward-backward asymmetry for positrons and  $K^-$  mesons

$$\begin{aligned} \frac{d^2 \bar{A}_{\text{FB}}^{(\text{Kl})}}{d\hat{q}^2 d\phi} &\equiv \int_{-1}^1 \text{sgn}(\cos \theta_l) d\cos \theta_l \\ &\times \int_{-1}^1 \text{sgn}(\cos \theta_K) d\cos \theta_K \mathcal{W}(\hat{q}^2, \theta_l, \theta_K, \phi) \\ &= -\frac{\sqrt{2}}{4\pi} \left( \text{Re}(a_0 a_{\parallel}^*) \cos \phi + \text{Im}(a_0 a_{\perp}^*) \sin \phi \right), \end{aligned} \quad (17)$$

will allow one to find  $\text{Re}(a_0 a_{\parallel}^*)$  and  $\text{Im}(a_0 a_{\perp}^*)$

$$A_5 \equiv \left( \int_0^{\pi/2} d\phi - \int_{\pi/2}^{3\pi/2} d\phi + \int_{3\pi/2}^{2\pi} d\phi \right) \frac{d^2 \bar{A}_{\text{FB}}^{(\text{Kl})}}{d\hat{q}^2 d\phi} = -\frac{\sqrt{2}}{\pi} \text{Re}(a_0 a_{\parallel}^*), \quad (18)$$

$$A_6 \equiv \left( \int_0^{\pi} d\phi - \int_{\pi}^{2\pi} d\phi \right) \frac{d^2 \bar{A}_{\text{FB}}^{(\text{Kl})}}{d\hat{q}^2 d\phi} = -\frac{\sqrt{2}}{\pi} \text{Im}(a_0 a_{\perp}^*). \quad (19)$$

Measurement of the azimuthal angle dependence of the forward-backward asymmetry for  $K^-$  mesons

$$\begin{aligned} \frac{d^2 \bar{A}_{\text{FB}}^{(\text{K})}}{d\hat{q}^2 d\phi} &\equiv \int_{-1}^1 d\cos \theta_l \int_{-1}^1 \text{sgn}(\cos \theta_K) d\cos \theta_K \mathcal{W}(\hat{q}^2, \theta_l, \theta_K, \phi) \\ &= -\frac{3\sqrt{2}}{16} \left( \text{Re}(a_{0L} a_{\perp L}^* - a_{0R} a_{\perp R}^*) \cos \phi \right. \\ &\quad \left. + \text{Im}(a_{0L} a_{\parallel L}^* - a_{0R} a_{\parallel R}^*) \sin \phi \right), \end{aligned} \quad (20)$$

will allow one to find  $\text{Re}(a_{0L} a_{\perp L}^* - a_{0R} a_{\perp R}^*)$  and  $\text{Im}(a_{0L} a_{\parallel L}^* - a_{0R} a_{\parallel R}^*)$

$$A_8 \equiv \left( \int_0^{\pi/2} d\phi - \int_{\pi/2}^{3\pi/2} d\phi + \int_{3\pi/2}^{2\pi} d\phi \right) \frac{d^2 \bar{A}_{\text{FB}}^{(\text{K})}}{d\hat{q}^2 d\phi} = -\frac{3\sqrt{2}}{4} \text{Re}(a_{0L} a_{\perp L}^* - a_{0R} a_{\perp R}^*), \quad (21)$$

$$\begin{aligned} A_9 &\equiv \left( \int_0^{\pi} d\phi - \int_{\pi}^{2\pi} d\phi \right) \frac{d^2 \bar{A}_{\text{FB}}^{(\text{K})}}{d\hat{q}^2 d\phi} \\ &= -\frac{3\sqrt{2}}{4} \text{Im}(a_{0L} a_{\parallel L}^* - a_{0R} a_{\parallel R}^*). \end{aligned} \quad (22)$$

### C. Transversity amplitudes

The nonresonant amplitudes follow from the matrix element of the  $\bar{B}_d^0(p) \rightarrow \bar{K}^{*0}(k, \epsilon) e^+(q_+) e^-(q_-)$  process in Eq. (A1),

$$A_{0L,R}^{\text{NR}} = \frac{C_0(q^2)}{2\hat{m}_{K^*}\sqrt{\hat{q}^2}} \left( C_{9V}^{\text{eff}} \mp C_{10A} + 2\hat{m}_b (C_{7\gamma}^{\text{eff}} - C_{7\gamma}'^{\text{eff}}) \kappa_0(q^2) \right), \quad (23)$$

$$A_{\parallel L,R}^{\text{NR}} = -\sqrt{2} C_{\parallel}(q^2) \left( C_{9V}^{\text{eff}} \mp C_{10A} + 2\frac{\hat{m}_b}{\hat{q}^2} (C_{7\gamma}^{\text{eff}} - C_{7\gamma}'^{\text{eff}}) \kappa_{\parallel}(q^2) \right), \quad (24)$$

$$A_{\perp L,R}^{\text{NR}} = \sqrt{2\hat{\lambda}} C_{\perp}(q^2) \left( C_{9V}^{\text{eff}} \mp C_{10A} + 2\frac{\hat{m}_b}{\hat{q}^2} (C_{7\gamma}^{\text{eff}} + C_{7\gamma}'^{\text{eff}}) \kappa_{\perp}(q^2) \right), \quad (25)$$

where the form factors enter as

$$C_0(q^2) = (1 - \hat{q}^2 - \hat{m}_{K^*}^2)(1 + \hat{m}_{K^*})A_1(q^2) - \hat{\lambda} \frac{A_2(q^2)}{1 + \hat{m}_{K^*}}, \quad (26)$$

$$C_{\parallel}(q^2) = (1 + \hat{m}_{K^*})A_1(q^2), \quad (27)$$

$$C_{\perp}(q^2) = \frac{V(q^2)}{1 + \hat{m}_{K^*}}, \quad (28)$$

$$\begin{aligned} \kappa_0(q^2) &\equiv \left( (1 - \hat{q}^2 + 3\hat{m}_{K^*}^2)(1 + \hat{m}_{K^*})T_2(q^2) \right. \\ &\quad \left. - \frac{\hat{\lambda}}{1 - \hat{m}_{K^*}} T_3(q^2) \right) \left( (1 - \hat{q}^2 - \hat{m}_{K^*}^2) \right. \\ &\quad \left. \times (1 + \hat{m}_{K^*})^2 A_1(q^2) - \hat{\lambda} A_2(q^2) \right)^{-1}, \end{aligned} \quad (29)$$

$$\kappa_{\parallel}(q^2) \equiv \frac{T_2(q^2)}{A_1(q^2)} (1 - \hat{m}_{K^*}), \quad (30)$$

$$\kappa_{\perp}(q^2) \equiv \frac{T_1(q^2)}{V(q^2)}(1 + \hat{m}_{K^*}). \quad (31)$$

In the above formulas the definition  $\hat{m}_b \equiv \bar{m}_b(\mu)/m_B$ ,  $\hat{m}_s \equiv \bar{m}_s(\mu)/m_B$  are used, and  $A_1(q^2)$ ,  $A_2(q^2)$ ,  $V(q^2)$ ,  $T_1(q^2)$ ,  $T_2(q^2)$ ,  $T_3(q^2)$  are the  $B \rightarrow K^*$  transition form factors, specified in Appendix A.

#### D. Resonant contribution

Next, we implement the effects of LD contributions from the decays  $\bar{B}_d^0 \rightarrow \bar{K}^{*0} V$ , where  $V = \rho^0, \omega, \phi, J/\psi(1S), \psi(2S), \dots$  mesons, followed by  $V \rightarrow e^+ e^-$  in the decay  $\bar{B}_d^0 \rightarrow \bar{K}^{*0} e^+ e^-$  (see Fig. 2). We ap-

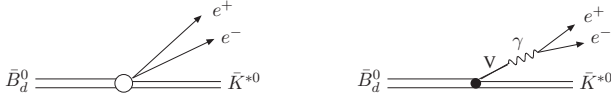


FIG. 2: Nonresonant and resonant contributions to the decay amplitude.

ply vector-meson dominance (VMD) approach. In general, the  $V \gamma$  transition can be included into consideration using various versions of VMD model. In the “standard” version (see, e.g. [19], chapter 6), the  $V \gamma$  transition vertex can be written as

$$\langle \gamma(q); \mu | V(q); \nu \rangle = -e f_V Q_V m_V g^{\mu\nu}, \quad (32)$$

where  $q$  is the virtual photon (vector meson) four-momentum,  $g^{\mu\nu}$  is the metric tensor,  $Q_V$  is the effective electric charge of the quarks in the vector meson:

$$Q_\rho = \frac{1}{\sqrt{2}}, \quad Q_\omega = \frac{1}{3\sqrt{2}}, \quad Q_\phi = -\frac{1}{3},$$

$$Q_{J/\psi} = Q_{\psi(2S)} = \dots = \frac{2}{3}. \quad (33)$$

The decay constants of neutral vector mesons  $f_V$  can be extracted from their electromagnetic decay width, using

$$\Gamma_{V \rightarrow e^+ e^-} = \frac{4\pi\alpha_{em}^2}{3m_V} f_V^2 Q_V^2. \quad (34)$$

This version of VMD model will be called VMD1. The vertex (32) comes from the transition Lagrangian

$$\mathcal{L}_{\gamma V} = -e A^\mu \sum_V f_V Q_V m_V V_\mu. \quad (35)$$

A more elaborate model (called hereafter VMD2) originates from Lagrangian

$$\mathcal{L}_{\gamma V} = -\frac{e}{2} F^{\mu\nu} \sum_V \frac{f_V Q_V}{m_V} V_{\mu\nu} \quad (36)$$

where  $V_{\mu\nu} \equiv \partial_\mu V_\nu - \partial_\nu V_\mu$  and  $F^{\mu\nu} \equiv \partial^\mu A^\nu - \partial^\nu A^\mu$  is the electromagnetic field tensor.

Lagrangian (36) is explicitly gauge invariant, unlike Eq. (35), and gives rise to the  $V \gamma^*$  vertex

$$\langle \gamma(q); \mu | V(q); \nu \rangle = -\frac{e f_V Q_V}{m_V} (q^2 g^{\mu\nu} - q^\mu q^\nu), \quad (37)$$

This transition vertex is suppressed at small invariant masses,  $q^2 \ll m_V^2$ , i.e. in the region far from the vector-meson mass shell [33].

Note that these two versions of the VMD model have been discussed in Refs. [20, 21]. The VMD2 version naturally follows from the Resonance Chiral Theory [22]; in this context VMD2 coupling has been applied in [23] for studying electron-positron annihilation into  $\pi^0 \pi^0 \gamma$  and  $\pi^0 \eta \gamma$  final states.

Parameters of vector resonances are presented in Table I.

TABLE I: Mass, total width, leptonic decay width and coupling  $f_V$  of vector mesons [24] (experimental uncertainties are not shown).

$V$	$m_V(\text{MeV})$	$\Gamma_V(\text{MeV})$	$\Gamma_{V \rightarrow e^+ e^-}(\text{keV})$	$f_V(\text{MeV})$
$\rho^0$	775.49	149.1	7.04	221.2
$\omega$	782.65	8.49	0.60	194.7
$\phi$	1019.455	4.26	1.27	228.6
$J/\psi$	3096.916	0.0929	5.55	416.4
$\psi(2S)$	3686.09	0.304	2.35	295.6
$\psi(3770)$	3772.92	27.3	0.265	100.4
$\psi(4040)$	4039	80	0.86	187.2
$\psi(4160)$	4153	103	0.83	186.5
$\psi(4415)$	4421	62	0.58	160.8

Based on VMD approach, we obtain the total amplitude including nonresonant and resonant parts,

$$A_{0L,R} = \frac{1}{2 \hat{m}_{K^*} \sqrt{\hat{q}^2}} \left( C_0(q^2) (C_{9V}^{\text{eff}} \mp C_{10A} + 2\hat{m}_b (C_{7\gamma}^{\text{eff}} - C_{7\gamma}'^{\text{eff}}) \kappa_0(q^2)) + 8\pi^2 \sum_V C_V D_V^{-1}(\hat{q}^2) \left( (1 - \hat{q}^2 - \hat{m}_{K^*}^2) S_1^V + \hat{\lambda} \frac{S_2^V}{2} \right) \right), \quad (38)$$

$$A_{\parallel L,R} = -\sqrt{2} \left( C_{\parallel}(q^2) (C_{9V}^{\text{eff}} \mp C_{10A} + 2\frac{\hat{m}_b}{\hat{q}^2} (C_{7\gamma}^{\text{eff}} - C_{7\gamma}'^{\text{eff}}) \kappa_{\parallel}(q^2)) + 8\pi^2 \sum_V C_V D_V^{-1}(\hat{q}^2) S_1^V \right), \quad (39)$$

$$\begin{aligned}
A_{\perp L,R} = & \sqrt{2\lambda} \left( C_{\perp}(q^2) (C_{9V}^{\text{eff}} \mp C_{10A}) \right. \\
& + 2 \frac{\hat{m}_b}{q^2} (C_{7\gamma}^{\text{eff}} + C_{7\gamma}'^{\text{eff}}) \kappa_{\perp}(q^2) \\
& \left. + 4\pi^2 \sum_V C_V D_V^{-1}(\hat{q}^2) S_3^V \right), \quad (40)
\end{aligned}$$

where

$$D_V(\hat{q}^2) = \hat{q}^2 - \hat{m}_V^2 + i\hat{m}_V \hat{\Gamma}_V(\hat{q}^2)$$

is the usual Breit-Wigner function for the  $V$  meson resonance shape with the energy-dependent width  $\Gamma_V(q^2)$  [ $\hat{\Gamma}_V(\hat{q}^2) = \Gamma_V(q^2)/m_B$ ],  $\hat{m}_V \equiv m_V/m_B$ ,  $\hat{\Gamma}_V \equiv \Gamma_V/m_B$ ,  $m_V(\Gamma_V)$  is the mass (width) of a  $V$  meson.

$$C_V = \frac{Q_V m_V f_V}{q^2} \text{ (VMD1)}, \quad C_V = \frac{Q_V f_V}{m_V} \text{ (VMD2)}. \quad (41)$$

In Eqs. (38)-(40),  $S_i^V$  ( $i = 1, 2, 3$ ) are the invariant amplitudes of the decay  $B_d^0 \rightarrow K^{*0} V$ . These amplitudes are calculated in Appendix B.

The energy-dependent widths of light vector resonances  $\rho$ ,  $\omega$  and  $\phi$  are chosen as in Ref. [15]. The updated branching ratios for resonances decays to different channels are taken from [24]. For the  $c\bar{c}$  resonances  $J/\psi$ ,  $\psi(2S)$ , ... we take the constant widths.

In order to calculate the resonant contribution to the amplitude of the  $\bar{B}_d^0 \rightarrow \bar{K}^{*0} e^+ e^-$  decay, one has to know the amplitudes of the decays  $\bar{B}_d^0 \rightarrow \bar{K}^{*0} \rho$ ,  $\bar{B}_d^0 \rightarrow \bar{K}^{*0} \omega$ ,  $\bar{B}_d^0 \rightarrow \bar{K}^{*0} \phi$ ,  $\bar{B}_d^0 \rightarrow \bar{K}^{*0} J/\psi$ ,  $\bar{B}_d^0 \rightarrow \bar{K}^{*0} \psi(2S)$ , ... At present the amplitudes of the  $\bar{B}_d^0 \rightarrow \bar{K}^{*0} \phi$ ,  $\bar{B}_d^0 \rightarrow \bar{K}^{*0} J/\psi$ ,  $\bar{B}_d^0 \rightarrow \bar{K}^{*0} \psi(2S)$  decays are known from experiment [24], therefore, we use these amplitudes for calculation of invariant amplitudes in Appendix B in Table VI. For the light resonances  $\rho$  and  $\omega$  we use the theoretical prediction [25] for the decay amplitudes. At the same time, we are not aware of a similar prediction for the higher  $c\bar{c}$  resonances, such as  $\psi(3770)$  and so on, therefore we do not include contribution of these resonances to amplitudes.

The parameters of the model are indicated in Table II. The SM Wilson coefficients have been obtained in [7] at the scale  $\mu = 4.8$  GeV to NNLO accuracy. In our notation (see Appendix A 1) these coefficients are given in Table III. In the numerical estimations, we use the form factors from the light-cone sum rules (LCSR) calculation [9].

### III. RESULTS OF THE CALCULATION FOR THE $\bar{B}_d^0 \rightarrow \bar{K}^{*0} e^+ e^-$ DECAY

#### A. Dependence of observables on dilepton invariant mass squared

In Figs. 3 we present results for the dependence of various observables in the  $\bar{B}_d^0 \rightarrow \bar{K}^{*0} e^+ e^-$  decay on

TABLE II: The numerical input used in our analysis.

$ V_{tb}V_{ts}^*  = 0.04026$	$G_F = 1.16637 \times 10^{-5} \text{ GeV}^{-2}$
$\mu = m_b = 4.8 \text{ GeV}$	$\alpha_{\text{em}} = 1/137.036$
$m_c = 1.4 \text{ GeV}$	$m_B = 5.27950 \text{ GeV}$
$\bar{m}_b(\mu) = 4.14 \text{ GeV}$	$\tau_B = 1.525 \text{ ps}$
$\bar{m}_s(\mu) = 0.079 \text{ GeV}$	$m_{K^*} = 0.89594 \text{ GeV}$

TABLE III: The SM Wilson coefficients at the scale  $\mu = 4.8$  GeV, to NNLO accuracy [7].

$\bar{C}_1(\mu)$	$\bar{C}_2(\mu)$	$\bar{C}_3(\mu)$	$\bar{C}_4(\mu)$	$\bar{C}_5(\mu)$
-0.128	1.052	0.011	-0.032	0.009
$\bar{C}_6(\mu)$	$C_{7\gamma}^{\text{eff}}(\mu)$	$C_{8g}^{\text{eff}}(\mu)$	$C_{9V}(\mu)$	$C_{10A}(\mu)$
-0.037	-0.304	-0.167	4.211	-4.103

the dilepton invariant mass squared. The interval of  $m_{ee} = \sqrt{q^2}$  is taken from 10 MeV to  $m_B - m_{K^*} \approx 4.384$  GeV. The phase  $\delta_0^V$  is chosen zero for all resonances except the  $\phi$  meson, for which  $\delta_0^\phi = 2.82$  rad (see Table VI).

As is seen in Fig. 3, predictions of VMD1 and VMD2 models differ for  $f_L$ ,  $A_{\text{FB}}$  and  $A_{\text{T}}^{(2)}$  at small  $q^2 \lesssim 2 \text{ GeV}^2$ , while for the differential branching at the bigger values,  $q^2 \gtrsim 8 \text{ GeV}^2$ . At the bigger values of invariant mass, VMD1 and VMD2 yield close results. Note that the difference between predictions of these two models is especially large for the high-lying resonances  $J/\psi$  and  $\psi(2S)$ .

In addition, VMD1 and VMD2 models lead to a qualitatively different behavior of longitudinal fraction  $f_L$  at small  $q^2$  (the upper right panel in Fig. 3). The data demonstrate that  $f_L \rightarrow 0$  at very small  $q^2$ , that is in agreement with calculation in the VMD2 model. In general, from comparison with data the VMD2 version seems somewhat more preferable.

Let us comment on the coefficient  $A_{\text{T}}^{(2)}$  in the azimuthal distribution (13), plotted in Fig. 3 (the lower right panel). According to the definition (14) and due to the properties of the  $K^*$  polarization fractions  $0 \leq f_{\parallel, \perp} \leq 1$ , the coefficient  $A_{\text{T}}^{(2)}$  is constrained:

$$-1 \leq A_{\text{T}}^{(2)} \leq 1. \quad (42)$$

The calculation in the SM with resonances yields the values of  $A_{\text{T}}^{(2)}$  which are much smaller than the data (see Fig. 3). In this connection we note that the experimental uncertainties are still big, and it is not clear if the measured  $q^2$ -dependence of  $A_{\text{T}}^{(2)}$  indeed lies in the limits (42).

It is seen from Fig. 3 (the upper left panel) that the charmonia resonances contribute to the differential branching far beyond their pole positions, especially in the VMD1 model. In order to investigate the role of the

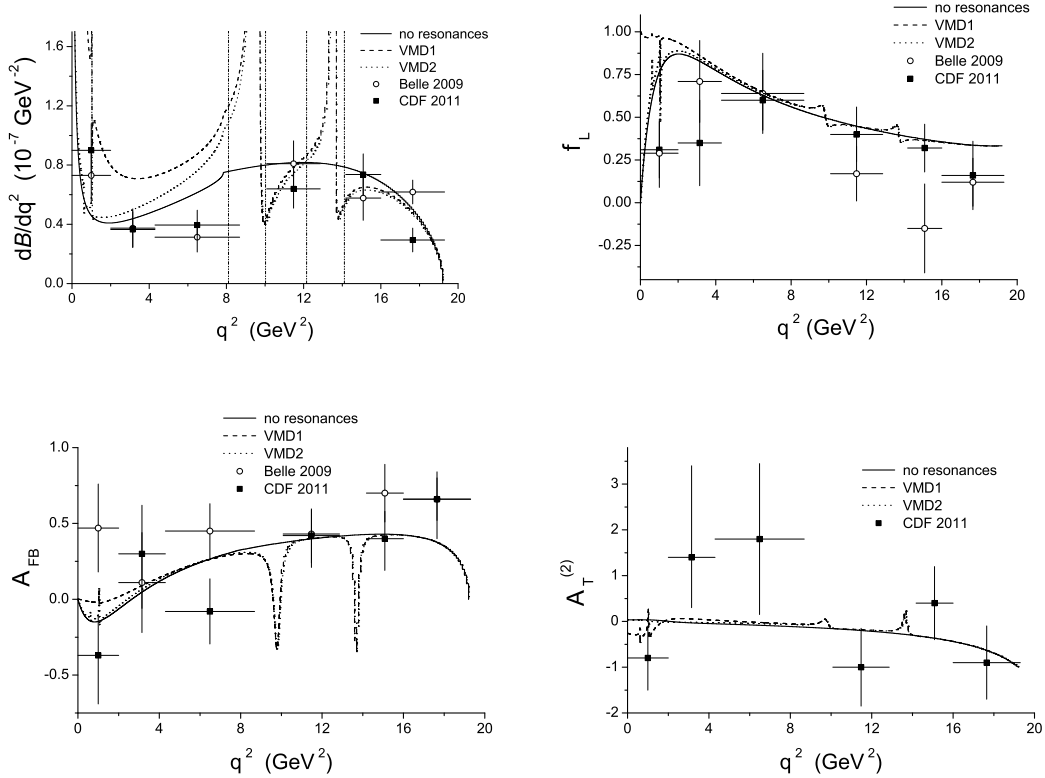


FIG. 3: The upper row: differential branching ratio (left), longitudinal polarization fraction of  $K^*$  meson (right); the lower row: forward-backward asymmetry  $A_{FB}$  (left), coefficient  $A_T^{(2)}$  (right) as functions of  $q^2$ . Solid line corresponds to the SM calculation without resonances taken into account. Dashed and dotted lines are calculated with account of resonances in the VMD1 and VMD2 versions of VMD model respectively. The form factors are taken from [9]. The data from Belle (KEKB) [12] and CDF (Tevatron) [13] are shown by the circles and boxes respectively. Due to the choice of reference frame in Fig. 1, the forward-backward asymmetry  $A_{FB}$  in Refs. [12, 13] is related to asymmetry in Eq. (12) via  $A_{FB} = -d\bar{A}_{FB}^{(l)}/dq^2$ . The dash-double-dot vertical lines in the figure for differential branching ratio indicate “charmonia veto” (see the text).

TABLE IV: Branching ratio for the decay  $\bar{B}_d^0 \rightarrow \bar{K}^{*0} e^+ e^-$  calculated within the limits:  $m_{ee}^{min} = 30$  MeV,  $m_{ee}^{max} = m_B - m_{K^*}$ . The 2nd column: for the whole interval of invariant mass, the 3rd column: with the “charmonia veto” (see the text).

model	BR ( $10^{-6}$ )	
	no veto	with veto
SM, no res.	1.32	1.01
SM, res. VMD1	134.2	49.6
SM, res. VMD2	85.6	1.03

charmonia resonances we calculate the total branching ratio in Table IV. Calculation over the whole allowed interval of invariant masses, shown in the 2nd column, demonstrates a very big resonance contribution.

Usually in experimental analyses [11–13] certain cuts

are applied in order to cut out the charmonia contributions (the so-called charmonia veto). In the 3rd column of Table IV we used the integration region with the following cut out intervals taken as in the BaBar analysis [11] for the  $e^+e^-$  pairs:  $8.11 \leq q^2 \leq 10.03$  GeV<sup>2</sup> and  $12.15 \leq q^2 \leq 14.11$  GeV<sup>2</sup>.

As is seen, the  $c\bar{c}$ -resonances contribution is completely eliminated. The result obtained in the VMD2 model becomes close (within a few percent) to the calculation without resonances. At the same time the VMD1 calculation still yields a big value of branching ratio, which is due to the steep rise of the differential branching at small invariant masses in Fig. 3.

The calculations, presented in Table IV, are the predictions of our model for the current experiments carried out at LHCb [14]. We can also compare predictions (with veto) in Table IV with experimental measurements:  $(1.07^{+0.11}_{-0.10} \pm 0.09) \times 10^{-6}$  for the  $B \rightarrow K^* \ell^+ \ell^-$  decay ( $\ell = e, \mu$ ) at Belle [12],  $(1.02 \pm 0.10 \pm 0.06) \times 10^{-6}$  for the  $B^0 \rightarrow K^{*0} \mu^+ \mu^-$  decay at CDF [13], and

$(1.02^{+0.30}_{-0.28} \pm 0.06) \times 10^{-6}$  for the  $B^0 \rightarrow K^{*0} e^+ e^-$  decay at BaBar [11].

In Figs. 4 we present asymmetries calculated according to Eqs. (14)–(16), (18), (19), (21), (22).

Asymmetry  $A_3 = \frac{1}{\pi}(1 - f_L)A_T^{(2)}$  takes sizable values at large invariant masses, while in the wide region of  $m_{ee}$  this observable is small, of the order of  $10^{-2}$  (see also Figs. 3 for  $A_T^{(2)}$ ). Account of resonances changes it mainly in the vicinity of the resonance positions, i.e. at  $m_{ee} \approx m_V$ .

As for  $A_5$  and  $A_8$ , they take sizable values in the whole region of  $q^2$  (see Figs. 4). The resonances give considerable contribution, especially to  $A_8$ . One of features is the point  $q_0^2$ , where these asymmetries cross zero. Calculation shows that the zero point,  $q_0^2 \sim 1.5 \text{ GeV}^2$ , is almost insensitive to the presence of the resonances. This feature makes these asymmetries convenient observables for experimental study, similarly to the forward-backward asymmetry  $A_{FB}$  in Fig. 3.

Some of the asymmetries are very small in the SM without resonances, in particular,  $A_9 \equiv 0$ ,  $A_4 \sim 10^{-4}$  and  $A_6 \sim 10^{-3}$  (Figs. 4). Note that these asymmetries are determined by the imaginary part of the bilinear combinations of the amplitudes. The imaginary part of the amplitudes in the SM (without resonances) is determined by the  $u, d, s$  and  $c$  quark loop through the function  $Y(q^2)$  [26], and therefore the imaginary part of the non-resonant amplitudes appears to be very small. Therefore in framework of the naive factorization, applied in the present work, it is not surprising that these asymmetries are small in the SM without resonances. Inclusion of the resonances changes behavior of these asymmetries in the wide region of invariant masses (see Figs. 4).

Recently the asymmetry  $A_{Im} = -\frac{\pi}{2}A_4$  in the  $B^0 \rightarrow K^{*0} \mu^+ \mu^-$  decay has been measured for the first time at CDF [13]. Note that the average values of this asymmetry over the  $q^2$ -ranges  $[0.0 - 4.3) \text{ GeV}^2$  and  $[1.0 - 6.0) \text{ GeV}^2$  are consistent with our calculations in framework of the SM.

One should note, that the amplitudes for the decay of  $B$  meson to two vector mesons are experimentally determined by the four polarization parameters, branching fraction and one overall phase  $\delta_0^V$  (the phase of the amplitude with zero helicity for decay  $B \rightarrow K^* V$ ). As it is seen from Eqs. (38)–(40) the contribution of resonances depends on the invariant amplitudes  $S_i^V$ . Values of these amplitudes are determined in Table VI, however their phases are defined with respect to the phase  $\delta_0^V$ , which is experimentally known only for the decay  $B \rightarrow K^* \phi$ . For other resonances, the phase  $\delta_0^V$  is not known either experimentally or theoretically.

As is seen in Figs. 4, the asymmetries  $A_4$  and  $A_9$  essentially depend on the choice of the  $\delta_0^{J/\psi}$  phase. Thus, in order to unambiguously determine the resonance contribution to the process  $\bar{B}_d^0 \rightarrow \bar{K}^{*0} (\rightarrow K^- \pi^+) \ell^+ \ell^-$ , the phases  $\delta_0^V$  should be known for all vector resonances  $\rho, \omega, \phi, J/\psi, \dots$ . These phases can be found from experi-

ments on  $B$ -meson decays through the interference with other  $B$  decays with the same final states, for example,  $B^0 \rightarrow \phi K^{*0}$  and  $B^0 \rightarrow \phi(K\pi)_0^{*0}$ , where  $(K\pi)_0^{*0}$  is the  $J^P = 0^+ K\pi$  component [27].

## B. Comparison of two approaches to including the resonances

Earlier in the literature [17] it has been suggested to combine the factorization assumption and VMD approximation in estimating LD effects for the  $B$  decays. This can be accomplished in an approximate manner through the substitution

$$C_{9V}^{\text{eff}} \rightarrow C_{9V}^{\text{eff}} - \frac{3\pi}{\alpha_{em}^2} C^{(0)} \sum_{\psi} k_{\psi} \frac{\hat{m}_{\psi} \hat{\Gamma}(\psi \rightarrow e^+ e^-)}{\hat{q}^2 - \hat{m}_{\psi}^2 + i \hat{m}_{\psi} \hat{\Gamma}_{\psi}}, \quad (43)$$

where the properties of the vector mesons  $\psi = J/\psi(1S), \psi(2S), \dots, \psi(4415)$  are summarized in Table I,  $\hat{\Gamma}_{\psi \rightarrow e^+ e^-} \equiv \Gamma_{\psi \rightarrow e^+ e^-} / m_B$ ,  $C^{(0)} = 3\bar{C}_1 + \bar{C}_2 + 3\bar{C}_3 + \bar{C}_4 + 3\bar{C}_5 + \bar{C}_6$ , and the Wilson coefficients are presented in Table III.

The last term in Eq. (43) describes the LD contribution of the real intermediate  $\bar{c}c$  states,  $k_{\psi} = |k_{\psi}| e^{i\delta_{\psi}}$  is the factor that the  $B \rightarrow K^* \psi$  amplitude, calculated using naive factorization, must be multiplied by to get the measured  $B \rightarrow K^* \psi$  rate. Under naive factorization, the branching ratio for  $B \rightarrow K^* \psi$  is

$$\begin{aligned} \text{BR}(B \rightarrow K^* \psi) &= m_B \tau_B \frac{\sqrt{\lambda(1, \hat{m}_{K^*}^2, \hat{m}_{\psi}^2)}}{16\pi} \\ &\times \left( \frac{G_F m_B^2}{\sqrt{2}} \right)^2 \left| V_{tb} V_{ts}^* \frac{C^{(0)}}{3} \right|^2 \\ &\times \left( |X_0^{\psi}|^2 + |X_{\parallel}^{\psi}|^2 + |X_{\perp}^{\psi}|^2 \right), \quad (44) \end{aligned}$$

where

$$\begin{aligned} X_0^{\psi} &= \frac{\hat{f}_{\psi}}{2\hat{m}_{K^*}(1 + \hat{m}_{K^*})} \left( (1 + \hat{m}_{K^*})^2 (1 - \hat{m}_{K^*}^2 \right. \\ &\left. - \hat{m}_{\psi}^2) A_1(m_{\psi}^2) - \lambda(1, \hat{m}_{K^*}^2, \hat{m}_{\psi}^2) A_2(m_{\psi}^2) \right), \quad (45) \end{aligned}$$

$$X_{\parallel}^{\psi} = -\sqrt{2} \hat{m}_{\psi} \hat{f}_{\psi} (1 + \hat{m}_{K^*}) A_1(m_{\psi}^2), \quad (46)$$

$$X_{\perp}^{\psi} = \sqrt{2} \lambda(1, \hat{m}_{K^*}^2, \hat{m}_{\psi}^2) \hat{m}_{\psi} \hat{f}_{\psi} / (1 + \hat{m}_{K^*}) V(m_{\psi}^2). \quad (47)$$

Here,  $\hat{f}_{\psi} \equiv f_{\psi}/m_B$ .

We calculate the values of  $k_{\psi}$  for each  $\bar{c}c$  resonance using experimental information from Tables I and VI and equation

$$|k_{\psi}|^2 = \frac{\text{BR}(B \rightarrow K^* \psi)_{\text{exp}}}{\text{BR}(B \rightarrow K^* \psi)_{\text{theor}}}. \quad (48)$$



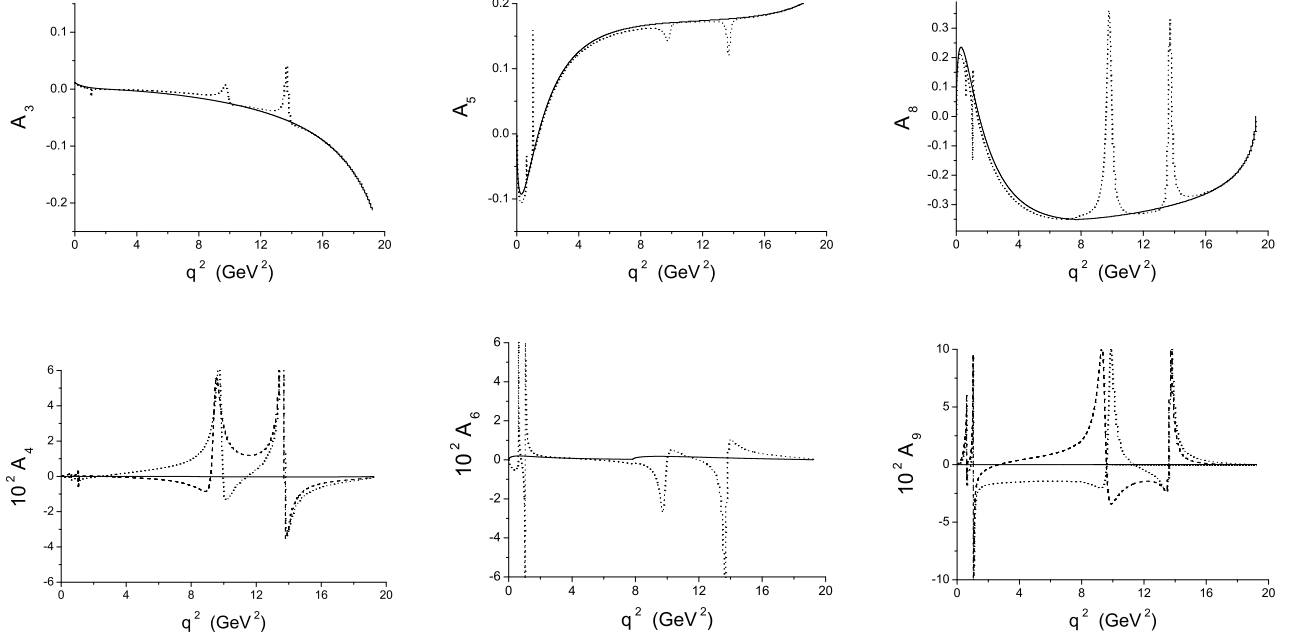


FIG. 4: Asymmetries as functions of  $q^2$ . The upper row from left to right:  $A_3$ ,  $A_5$  and  $A_8$ ; the lower row from left to right:  $A_4$ ,  $A_6$  and  $A_9$ . Solid lines correspond to the SM calculation without resonances, dotted (dashed) lines correspond to calculation including resonances with the zero-helicity phase  $\delta_0^{J/\psi} = 0$  ( $\delta_0^{J/\psi} = 2.45$  rad). Calculation is performed in the VMD2 version.

Using the form factors  $A_1$ ,  $A_2$ ,  $V$  in the LCSR model [9] we find the values:  $|k_{J/\psi}| = 0.894$ ,  $|k_{\psi(2S)}| = 0.841$  and for the higher resonances the average of the  $|k_{J/\psi}|$  and  $|k_{\psi(2S)}|$  is used. The phase of  $k_\psi$  is chosen zero as in the factorization approach. Note, that the above values of the parameters  $k_\psi$  are considerably smaller than the values used in the earlier papers [4, 16, 17]. Therefore we can expect the smaller resonance contribution to the differential branching and forward-backward asymmetry as compared with results of these papers.

Using Eqs. (43), (23)–(25) we calculate the observables for the  $\bar{B}_d^0 \rightarrow \bar{K}^{*0} e^+ e^-$  decay. These results are compared with results of calculations performed in the previous sections, in which only  $J/\psi$  and  $\psi(2S)$  resonances are included. This comparison may show sensitivity of the branching,  $K^*$  polarization fractions and asymmetries to the method of including the vector resonances.

Firstly, from Fig. 5 one sees that the two ways of including the resonances give very close predictions for differential branching, forward-backward asymmetry and asymmetry  $A_8$  in the region of  $q^2$  up to  $m_{\psi(2S)}^2$ . Note, that calculations of the branching and forward-backward asymmetry have been performed in Ref. [4] using formulas analogous to Eqs. (43). Our results in Figs. 5 qualitatively agree with calculations in [4].

Secondly, in Fig. 6 we present asymmetries, which strongly depend on the method of including resonances. As for asymmetries  $A_T^{(2)}$  and  $A_5$ , these two methods give essentially different predictions in the region of res-

onances  $J/\psi$  and  $\psi(2S)$ , while far from the resonance region, the predictions coincide with the non-resonant calculations. In the other asymmetries,  $A_4$ ,  $A_6$  and  $A_9$ , the two methods give different predictions not only in the resonance region but also at  $q^2$  away from resonances.

#### IV. CONCLUSIONS

The rare FCNC decay  $\bar{B}_d^0 \rightarrow \bar{K}^{*0} (\rightarrow K^- \pi^+) e^+ e^-$  has been studied in the whole region of electron-positron invariant masses up to  $m_B - m_{K^*}$ . The fully differential angular distribution over the three angles and dilepton invariant mass for the four-body decay  $\bar{B}_d^0 \rightarrow K^- \pi^+ e^+ e^-$  is analyzed. We defined a convenient set of asymmetries which allows one to extract them from measurement of the angular distribution once sufficient statistics is accumulated. We performed calculations of the differential branching ratio, polarization fractions of  $K^*$  meson and asymmetries. These asymmetries may have sensitivity to various effects of NP, although in order to see signatures of these effects the resonance contribution should be accurately estimated.

Contribution of the intermediate vector resonances in the process  $\bar{B}_d^0 \rightarrow \bar{K}^{*0} (\rightarrow K^- \pi^+) V$  with  $V = \rho(770)$ ,  $\omega(782)$ ,  $\phi(1020)$ ,  $J/\psi$ ,  $\psi(2S)$ , decaying into the  $e^+ e^-$  pair, has been taken into account. Various aspects of theoretical treatment of this long-distance contribution have been studied.

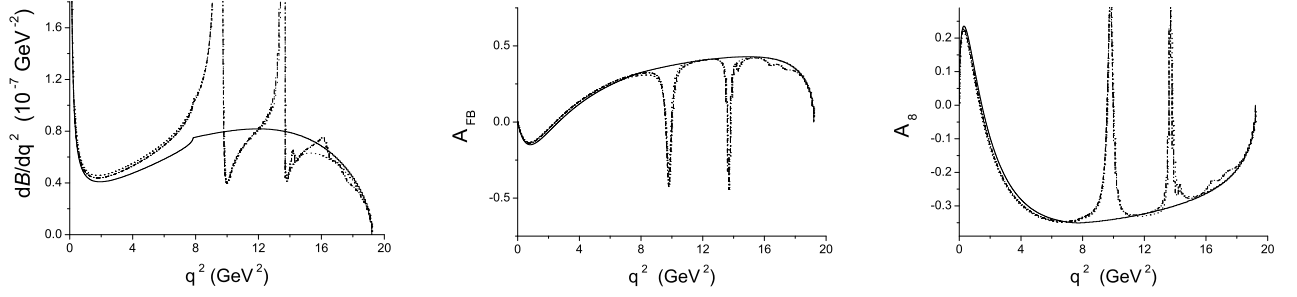


FIG. 5: Differential branching (left), forward-backward asymmetry (middle) and asymmetry  $A_8$  (right) a function of  $q^2$ . Solid lines are calculated without resonances, dotted lines are calculated with resonances  $J/\psi$ ,  $\psi(2S)$  according Eqs. (38)–(40), and dash-dotted lines with resonances according to Eqs. (43), (23)–(25).

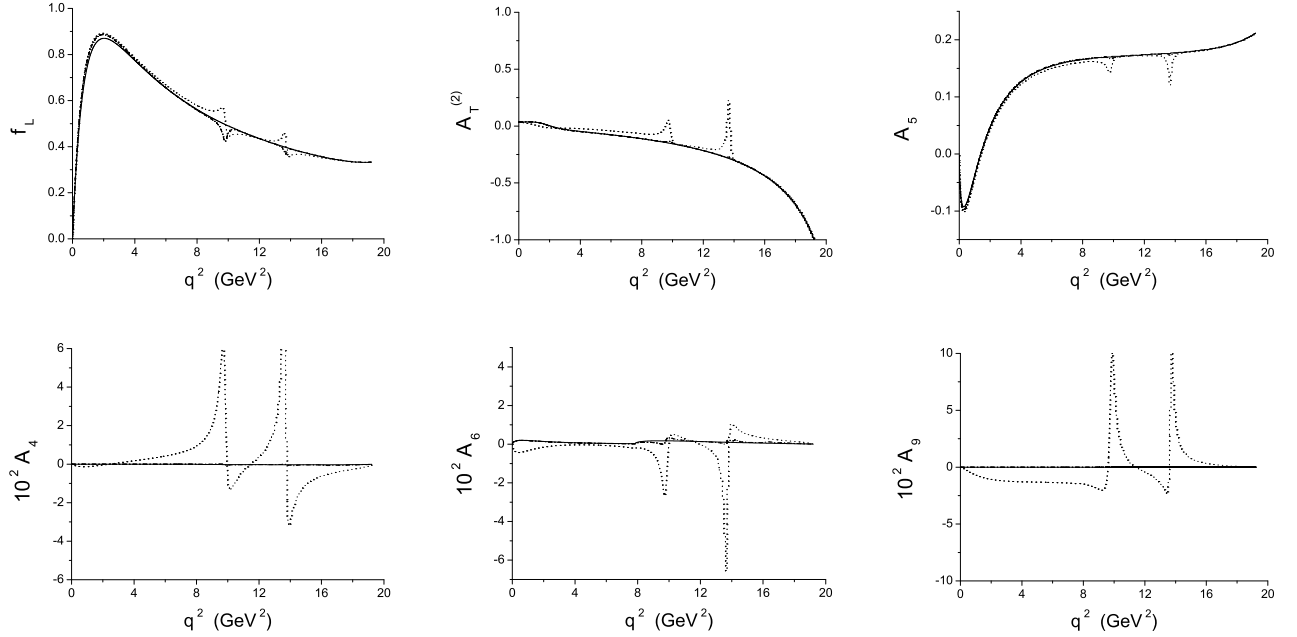


FIG. 6: The upper row from left to right: longitudinal polarization fraction  $f_L$ , asymmetries  $A_T^{(2)}$  and  $A_5$ ; the lower row from left to right: asymmetries  $A_4$ ,  $A_6$  and  $A_9$ , as functions of  $q^2$ . Solid lines are calculated without resonances, dotted lines are calculated with resonances  $J/\psi$ ,  $\psi(2S)$  according Eqs. (38)–(40), and dash-dotted lines with resonances according to Eqs. (43), (23)–(25).

The important aspect is the choice of the VMD model, describing the  $V\gamma$  transition. We used two variants of the VMD model, called here VMD1 and VMD2 versions, in particular, the VMD2 one is explicitly gauge-invariant and yields a  $V\gamma$  vertex which is suppressed at small values of the photon invariant mass far from the vector-meson mass shell. This is especially important in the treatment of the high-lying  $J/\psi$  and other  $c\bar{c}$  resonances at values  $q^2 \ll m_V^2$ . Some of the observables appeared to be rather sensitive to the choice of the  $V\gamma$  vertex. Based on comparison of calculation with the recent data from Belle and CDF experiments we can conclude that

the VMD2 version is somewhat more preferable.

For the vertex  $\bar{B}_d^0 \rightarrow \bar{K}^{*0} V$  we used an off-mass-shell extension of the helicity amplitudes describing production of on-shell vector mesons. For the latter the experimental information is used if available, and otherwise theoretical predictions.

The total branching ratio of the decay  $\bar{B}_d^0 \rightarrow \bar{K}^{*0} e^+ e^-$  in the interval  $30 \text{ MeV} \leq m_{ee} \leq m_B - m_{K^*}$  is calculated, and the resonance contribution is evaluated. The latter appeared to be very big, as expected. The calculated branching is  $\text{BR} = 1.32 \times 10^{-6}$  ( $85.6 \times 10^{-6}$ ) without resonances (with resonances in VMD2 version). To cut out

the  $c\bar{c}$ -resonance contribution, we also applied the “charmonia veto” as is usually done in experimental analyses [11–13]. Then our prediction for the total branching becomes  $\text{BR} = 1.01 \times 10^{-6}$  ( $1.03 \times 10^{-6}$ ) for the SM calculation without resonances (with resonances in VMD2 model).

All asymmetries are calculated in the whole region of invariant masses. The polarization asymmetry  $A_T^{(2)}$  (and  $A_3 = \frac{1}{\pi}(1 - f_L)A_T^{(2)}$ ) takes sizable values only at large  $m_{ee}$ . Account of resonances changes  $A_T^{(2)}$  mainly in the vicinity of the resonances, i.e. at  $m_{ee} \approx m_V$ . The asymmetries  $A_5$  and  $A_8$  take big values in the whole region of  $q^2$ , and resonances noticeably contribute, especially to  $A_8$ . An interesting feature of these asymmetries is their crossing zero at some  $q_0^2$ . This zero point,  $q_0^2 \sim 1.5 \text{ GeV}^2$ , turns out to be almost independent of the presence of resonances, and this property makes these asymmetries convenient observables for experimental study, similarly to the forward-backward asymmetry  $A_{\text{FB}}$ .

Some of the asymmetries are very small in the SM without resonances, in particular,  $A_9 \equiv 0$ ,  $A_4 \sim 10^{-4}$  and  $A_6 \sim 10^{-3}$ ; inclusion of the resonances changes behavior of these asymmetries considerably.

Our calculations are compared with recent data [12, 13] for  $q^2$ -dependence of the differential branching ratio, longitudinal polarization fraction of  $K^*$ , forward-backward asymmetry  $A_{\text{FB}}$  and transverse asymmetry  $A_T^{(2)}$ . On the whole, results of calculation are in reasonable agreement with the data.

We also compared predictions of our method with other existing in the literature method of including the  $c\bar{c}$  resonances through a modification of the Wilson coefficient  $C_{9V}^{\text{eff}}$  [17]. Our calculation shows that a few observables (differential branching ratio, forward-backward asymmetry and asymmetry  $A_8$ ) are independent of the calculation method, if the parameters  $|k_\psi|$  in Eq. (43) are equal to: 0.894 for  $J/\psi$ , 0.841 for  $\psi(2S)$  and 0.8675 for the higher  $c\bar{c}$  resonances. The phase of  $k_\psi$  is chosen zero. These values are considerably smaller than the values used in [4, 16, 17].

At the same time there exist asymmetries, predictions for which are substantially different in these two methods, namely,  $A_T^{(2)}$ ,  $A_5$  are different in the vicinity of resonances  $J/\psi$  and  $\psi(2S)$ , while  $A_4$ ,  $A_6$ ,  $A_9$  are different in the whole region of invariant masses. Thus measurement of the latter asymmetries may also be useful for selecting a more adequate method of including the long-distance resonance contribution to the  $\bar{B}_d^0 \rightarrow \bar{K}^{*0} (\rightarrow K^- \pi^+) \ell^+ \ell^-$  decay.

Calculations performed in the present work may be useful for experiments aiming at search of effects of the NP in the decay  $\bar{B}_d^0 \rightarrow \bar{K}^{*0} (\rightarrow K^- \pi^+) \ell^+ \ell^-$ .

## Appendix A: Matrix element and form factors

### 1. Matrix element

The effective Hamiltonian for the quark-level transition  $b \rightarrow s e^+ e^-$  within the SM is well-known and can be taken, e.g., from Ref. [1]. It is expressed in terms of the local operators  $\mathcal{O}_i$  and Wilson coefficients  $C_i$ , where  $i = 1, \dots, 6, 7\gamma, 8g, 9V, 10A$ .

The matrix element of this effective Hamiltonian for the nonresonant decay  $\bar{B}_d^0(p) \rightarrow \bar{K}^{*0}(k, \epsilon) e^+(q_+) e^-(q_-)$  can be written, in the so-called naive factorization [1], as

$$\begin{aligned} \mathcal{M}_{\text{NR}} = & \frac{G_F \alpha_{\text{em}}}{\sqrt{2}\pi} V_{ts}^* V_{tb} \left( \langle \bar{K}^{*0}(k, \epsilon) | \bar{s} \gamma_\mu P_L b | \bar{B}_d^0(p) \rangle \right. \\ & \times (C_{9V}^{\text{eff}} \bar{u}(q_-) \gamma^\mu v(q_+) + C_{10A} \bar{u}(q_-) \gamma^\mu \gamma_5 v(q_+)) \\ & - \frac{2}{q^2} \bar{m}_b(\mu) \langle \bar{K}^{*0}(k, \epsilon) | \bar{s} i \sigma_{\mu\nu} q^\nu (C_{7\gamma}^{\text{eff}} P_R \\ & \left. + C_{7\gamma}'^{\text{eff}} P_L) b | \bar{B}_d^0(p) \rangle \bar{u}(q_-) \gamma^\mu v(q_+) \right). \end{aligned} \quad (\text{A1})$$

Here,  $P_{L,R} = (1 \mp \gamma_5)/2$  denote chiral projectors, and  $\bar{m}_b(\mu)$  [ $\bar{m}_s(\mu)$ ] is the running bottom (strange) quark mass in the  $\overline{\text{MS}}$  scheme at the scale  $\mu$ . Moreover,  $\sigma_{\mu\nu} = \frac{i}{2}[\gamma_\mu, \gamma_\nu]$ ,  $q_\mu = (q_+ + q_-)_\mu$ ,  $C_{7\gamma}^{\text{eff}} = C_{7\gamma} - (4\bar{C}_3 - \bar{C}_5)/9 - (4\bar{C}_4 - \bar{C}_6)/3$ ,  $C_{9V}^{\text{eff}} = C_{9V} + Y(q^2)$ , where  $Y(q^2)$  is given in Ref. [26]. Note that in the framework of the SM  $\bar{m}_b(\mu) C_{7\gamma}'^{\text{eff}} = \bar{m}_s(\mu) C_{7\gamma}^{\text{eff}}$ .

The “barred” coefficients  $\bar{C}_i$  (for  $i = 1, \dots, 6$ ) are defined as certain linear combinations of the  $C_i$ , such that the  $\bar{C}_i$  coincide at leading logarithmic order with the Wilson coefficients in the standard basis [28]. The coefficients  $C_i$  are calculated at the scale  $\mu = m_W$ , in a perturbative expansion in powers of  $\alpha_s(m_W)$ , and are then evolved down to scales  $\mu \sim m_b$  using the renormalization group equations.

The  $\overline{\text{MS}}$  masses  $\bar{m}_b(\mu)$  and  $\bar{m}_s(\mu)$  are calculated according to Refs. [29, 30] and are given in Table II.

### 2. Form factors of $B \rightarrow K^*$ transition

The hadronic part of the matrix element in Eq. (A1) describing the  $B \rightarrow K^* e^+ e^-$  transition can be parametrized in terms of  $B \rightarrow K^*$  form factors, which usually are defined as

$$\langle \bar{K}^*(k, \epsilon) | \bar{s} \gamma_\mu b | \bar{B}(p) \rangle = \frac{2V(q^2)}{m_B + m_{K^*}} \varepsilon_{\mu\nu\alpha\beta} \epsilon^{\nu*} p^\alpha k^\beta, \quad (\text{A2})$$

$$\begin{aligned} \langle \bar{K}^*(k, \epsilon) | \bar{s} \gamma_\mu \gamma_5 b | \bar{B}(p) \rangle = & i\epsilon_\mu^*(m_B + m_{K^*}) A_1(q^2) \\ & - i(\epsilon^* \cdot p)(p + k)_\mu \frac{A_2(q^2)}{m_B + m_{K^*}} \\ & - i(\epsilon^* \cdot p) q_\mu \frac{2m_{K^*}}{q^2} \\ & \times (A_3(q^2) - A_0(q^2)), \end{aligned} \quad (\text{A3})$$

TABLE V: The parameters  $r_{1,2}$ ,  $m_R^2$ , and  $m_{fit}^2$  describing the  $q^2$  dependence of the  $B \rightarrow K^*$  form factors in the LCSR approach [9] and  $T_3(q^2) = \frac{m_B^2 - m_{K^*}^2}{q^2} (\tilde{T}_3(q^2) - T_2(q^2))$ . The fit equations to be used are given in the last column.

	$r_1$	$r_2$	$m_R^2, \text{GeV}^2$	$m_{fit}^2, \text{GeV}^2$	Fit eq.
$V$	0.923	-0.511	$(5.32)^2$	49.40	(A6)
$A_1$		0.290		40.38	(A8)
$A_2$	-0.084	0.342		52.00	(A7)
$A_0$	1.364	-0.990	$(5.28)^2$	36.78	(A6)
$T_1$	0.823	-0.491	$(5.32)^2$	46.31	(A6)
$T_2$		0.333		41.41	(A8)
$\tilde{T}_3$	-0.036	0.368		48.10	(A7)

with

$$A_3(q^2) = \frac{m_B + m_{K^*}}{2 m_{K^*}} A_1(q^2) - \frac{m_B - m_{K^*}}{2 m_{K^*}} A_2(q^2),$$

$$A_0(0) = A_3(0);$$

$$\langle \bar{K}^*(k, \epsilon) | \bar{s} \sigma_{\mu\nu} q^\nu b | \bar{B}(p) \rangle = i 2 T_1(q^2) \varepsilon_{\mu\nu\alpha\beta} \epsilon^{\nu*} p^\alpha k^\beta, \quad (\text{A4})$$

$$\begin{aligned} \langle \bar{K}^*(k, \epsilon) | \bar{s} \sigma_{\mu\nu} \gamma_5 q^\nu b | \bar{B}(p) \rangle \\ = T_2(q^2) (\epsilon_\mu^* (P \cdot q) - (\epsilon^* \cdot q) P_\mu) \\ + T_3(q^2) (\epsilon^* \cdot q) (q_\mu - \frac{q^2}{P \cdot q} P_\mu), \end{aligned} \quad (\text{A5})$$

with  $T_1(0) = T_2(0)$ . In the above equations,  $q = p - k$ ,  $P = p + k$ ,  $p^2 = m_B^2$ ,  $k^2 = m_{K^*}^2$ ,  $\epsilon^\mu$  is the polarization vector of the  $K^*$  meson,  $\epsilon^* \cdot k = 0$ , and  $\varepsilon_{0123} = 1$ .

The  $q^2$  dependence of the  $B \rightarrow K^*$  form factors given in [9] is parametrized as

$$F(q^2) = \frac{r_1}{1 - q^2/m_R^2} + \frac{r_2}{1 - q^2/m_{fit}^2}, \quad (\text{A6})$$

$$F(q^2) = \frac{r_1}{1 - q^2/m_{fit}^2} + \frac{r_2}{(1 - q^2/m_{fit}^2)^2}, \quad (\text{A7})$$

$$F(q^2) = \frac{r_2}{1 - q^2/m_{fit}^2}, \quad (\text{A8})$$

where the fit parameters  $r_{1,2}$ ,  $m_R^2$ , and  $m_{fit}^2$  are shown in Table V.

## Appendix B: Amplitudes of $B \rightarrow K^* V$ decays

An important ingredient of the resonant contribution is amplitude of the decay of  $B$  meson into two vector

mesons,  $B(p) \rightarrow V_1(q, \epsilon_1) + V_2(k, \epsilon_2)$ , with on-mass-shell meson  $V_2$  ( $k^2 = m_2^2$ ) and off-mass-shell meson  $V_1$  ( $q^2 \neq m_1^2$ ).

For the case of two on-mass-shell final mesons one can write the amplitude in the form [31]

$$\begin{aligned} \mathcal{M} = & \frac{G_F m_B^3}{\sqrt{2}} |V_{CKM}| \left( S_1 g_{\mu\nu} + \frac{S_2}{m_B^2} p_\mu p_\nu \right. \\ & \left. - i \frac{S_3}{m_B^2} \varepsilon_{\mu\nu\alpha\beta} q^\alpha k^\beta \right) \epsilon_1^{\mu*} \epsilon_2^{\nu*} \end{aligned} \quad (\text{B1})$$

in terms of three invariant amplitudes  $S_1$ ,  $S_2$  and  $S_3$ ,  $V_{CKM}$  is a CKM factor. The quantities  $S_1$ ,  $S_2$  and  $S_3$  may be complex and involve two types of phases,  $CP$ -conserving strong phases and  $CP$ -violating weak phases. In general, the invariant amplitudes are a sum of several interfering amplitudes,  $S_{1j}$ ,  $S_{2j}$  and  $S_{3j}$ , respectively. Then the phase structure of  $S_1$ ,  $S_2$  and  $S_3$  is:

$$S_k = \sum_j |S_{kj}| e^{i\varphi_{kj}} e^{i\delta_{kj}} \quad (k = 1, 2, 3), \quad (\text{B2})$$

where  $\varphi_{1j}$ ,  $\varphi_{2j}$ , and  $\varphi_{3j}$  are the  $CP$ -violating weak phases and  $\delta_{1j}$ ,  $\delta_{2j}$ , and  $\delta_{3j}$  are the  $CP$ -conserving strong phases.

Using  $CPT$  invariance, we can represent the matrix element for the charge-conjugate decay  $\bar{B}(p) \rightarrow \bar{V}_1(q, \epsilon_1) \bar{V}_2(k, \epsilon_2)$  as

$$\begin{aligned} \bar{\mathcal{M}} = & \frac{G_F m_B^3}{\sqrt{2}} |V_{CKM}^*| \left( \bar{S}_1 g_{\mu\nu} + \frac{\bar{S}_2}{m_B^2} p_\mu p_\nu \right. \\ & \left. + i \frac{\bar{S}_3}{m_B^2} \varepsilon_{\mu\nu\alpha\beta} q^\alpha k^\beta \right) \epsilon_1^{\mu*} \epsilon_2^{\nu*}, \end{aligned} \quad (\text{B3})$$

where  $\bar{S}_1$ ,  $\bar{S}_2$ , and  $\bar{S}_3$  can be derived from  $S_1$ ,  $S_2$ , and  $S_3$  by reversing the sign of the  $CP$ -violating phase. Note that if the  $B \rightarrow V_1 V_2$  decay is invariant under the  $CP$  symmetry, then  $\bar{S}_1 = S_1$ ,  $\bar{S}_2 = S_2$ , and  $\bar{S}_3 = S_3$ . On the other hand, if all  $CP$ -conserving phases of invariant amplitudes are equal to zero, then  $\bar{S}_1 = S_1^*$ ,  $\bar{S}_2 = S_2^*$ , and  $\bar{S}_3 = S_3^*$ .

The helicity amplitudes in terms of three invariant amplitudes,  $S_1$ ,  $S_2$ , and  $S_3$  are:

$$\begin{aligned} H_\lambda \equiv & \left( S_1 g_{\mu\nu} + \frac{S_2}{m_B^2} p_\mu p_\nu \right. \\ & \left. - i \frac{S_3}{m_B^2} \varepsilon_{\mu\nu\alpha\beta} q^\alpha k^\beta \right) \epsilon_1^{\mu*}(\lambda) \epsilon_2^{\nu*}(\lambda). \end{aligned} \quad (\text{B4})$$

From the decomposition Eq. (B4) one finds the following relations between the helicity amplitudes and the invariant amplitudes  $S_1$ ,  $S_2$ ,  $S_3$ :

$$\begin{aligned} H_0 = & -\frac{1}{2\hat{m}_1\hat{m}_2} \left( (1 - \hat{m}_1^2 - \hat{m}_2^2) S_1 \right. \\ & \left. + \frac{S_2}{2} \lambda(1, \hat{m}_1^2, \hat{m}_2^2) \right), \\ H_\pm = & S_1 \pm \frac{S_3}{2} \sqrt{\lambda(1, \hat{m}_1^2, \hat{m}_2^2)}, \end{aligned} \quad (\text{B5})$$

with  $\lambda(1, \hat{m}_1^2, \hat{m}_2^2) \equiv (1 - \hat{m}_1^2)^2 - 2\hat{m}_2^2(1 + \hat{m}_1^2) + \hat{m}_2^4$  and  $\hat{m}_{1(2)} \equiv m_{1(2)}/m_B$ .

Note that the polarized decay amplitudes can be expressed in several different but equivalent bases. For example, the helicity amplitudes can be related to the spin amplitudes in the transversity basis ( $A_0, A_{\parallel}, A_{\perp}$ ) defined in terms of the linear polarization of the vector mesons via:

$$A_0 = H_0, \quad A_{\parallel} = \frac{H_+ + H_-}{\sqrt{2}}, \quad A_{\perp} = \frac{H_+ - H_-}{\sqrt{2}}, \quad (\text{B6})$$

$A_0, A_{\parallel}, A_{\perp}$  are related to  $S_1, S_2$  and  $S_3$  of Eq. (B1) via

$$\begin{aligned} A_0 &= -\frac{1}{2\hat{m}_1\hat{m}_2} \left( (1 - \hat{m}_1^2 - \hat{m}_2^2) S_1 \right. \\ &\quad \left. + \frac{S_2}{2} \lambda(1, \hat{m}_1^2, \hat{m}_2^2) \right), \\ A_{\parallel} &= \sqrt{2} S_1, \quad A_{\perp} = \sqrt{\frac{\lambda(1, \hat{m}_1^2, \hat{m}_2^2)}{2}} S_3. \end{aligned} \quad (\text{B7})$$

The amplitude  $\bar{A}_{\lambda}$  ( $\lambda = 0, \parallel, \perp$ ) are related to the invariant amplitudes of the  $\bar{B} \rightarrow \bar{V}_1 \bar{V}_2$  decay by the formulas

$$\begin{aligned} \bar{A}_0 &= -\frac{1}{2\hat{m}_1\hat{m}_2} \left( (1 - \hat{m}_1^2 - \hat{m}_2^2) \bar{S}_1 \right. \\ &\quad \left. + \frac{\bar{S}_2}{2} \lambda(1, \hat{m}_1^2, \hat{m}_2^2) \right), \\ \bar{A}_{\parallel} &= \sqrt{2} \bar{S}_1, \quad \bar{A}_{\perp} = -\sqrt{\frac{\lambda(1, \hat{m}_1^2, \hat{m}_2^2)}{2}} \bar{S}_3. \end{aligned} \quad (\text{B8})$$

If the  $B \rightarrow V_1 V_2$  decay is invariant under  $CP$  transformation, then  $\bar{A}_0 = A_0$ ,  $\bar{A}_{\parallel} = A_{\parallel}$ , and  $\bar{A}_{\perp} = -A_{\perp}$ .

The decay width is expressed as follows:

$$\begin{aligned} \Gamma(B \rightarrow V_1 V_2) &= \frac{m_B \sqrt{\lambda(1, \hat{m}_1^2, \hat{m}_2^2)}}{16\pi} \left( \frac{G_F m_B^2}{\sqrt{2}} |V_{CKM}| \right)^2 \\ &\quad \times (|A_0|^2 + |A_{\parallel}|^2 + |A_{\perp}|^2). \end{aligned} \quad (\text{B9})$$

The matrix element for the  $B_d^0 \rightarrow K^{*0} V$  decay, where  $V = \rho^0, \omega, \phi, J/\psi(1S), \psi(2S), \dots$  mesons, we can represent as

$$\begin{aligned} \mathcal{M} &= \frac{G_F m_B^3}{\sqrt{2}} |V_{tb}^* V_{ts}| \left( S_1^V g_{\mu\nu} + \frac{S_2^V}{m_B^2} p_{\mu} p_{\nu} \right. \\ &\quad \left. - i \frac{S_3^V}{m_B^2} \varepsilon_{\mu\nu\alpha\beta} q^{\alpha} k^{\beta} \right) \epsilon_1^{\mu*} \epsilon_2^{\nu*}. \end{aligned} \quad (\text{B10})$$

Next, we define the normalized amplitudes:

$$h_{\lambda} \equiv \frac{A_{\lambda}}{\sqrt{\sum_{\lambda'} |A_{\lambda'}|^2}}, \quad \sum_{\lambda} |h_{\lambda}|^2 = 1 \quad (\lambda, \lambda' = 0, \parallel, \perp). \quad (\text{B11})$$

By putting  $m_1 = m_V$ ,  $m_2 = m_{K^*}$  and using (B9), (B11) we obtain the relation between the amplitudes  $h_{\lambda}$  and  $A_{\lambda}$  of the process under study  $B_d^0 \rightarrow K^{*0} V$  for any vector meson  $V = \rho^0, \omega, \phi, J/\psi(1S), \psi(2S), \dots$ :

$$\begin{aligned} h_{\lambda}^V &= \frac{G_F m_B^2}{4\sqrt{2}} |V_{tb}^* V_{ts}| \sqrt{\frac{m_B \tau_B}{\pi \text{BR}(B_d^0 \rightarrow K^{*0} V)}} \\ &\quad \times \lambda^{1/4}(1, \hat{m}_V^2, \hat{m}_{K^*}^2) A_{\lambda}^V, \end{aligned} \quad (\text{B12})$$

where  $\text{BR}(\dots)$  is the branching ratio of  $B_d^0 \rightarrow K^{*0} V$  decay and  $\tau_B$  is the lifetime of a  $B$  meson.

Solving Eqs. (B7) we find the scalars  $S_1, S_2$  and  $S_3$ , and then extend the helicity amplitudes  $A_{\lambda}^V$  off the mass shell of the meson  $V$ , i.e. for  $q^2 \neq m_V^2$ . We introduce the phases  $\delta_{\lambda}^V \equiv \arg(h_{\lambda}^V)$ ,  $\delta_i^V \equiv \arg(S_i^V)$ , where  $i = 1, 2, 3$ . Then we have

$$\begin{aligned} |S_1^V| &= \frac{|A_{\parallel}^V|}{\sqrt{2}}, \quad |S_3^V| = \sqrt{\frac{2}{\lambda(1, \hat{m}_V^2, \hat{m}_{K^*}^2)}} |A_{\perp}^V|, \\ |S_2^V| &= \frac{\sqrt{2}}{\lambda(1, \hat{m}_V^2, \hat{m}_{K^*}^2)} \left( 8\hat{m}_{K^*}^2 \hat{m}_V^2 |A_0^V|^2 \right. \\ &\quad \left. + (1 - \hat{m}_V^2 - \hat{m}_{K^*}^2)^2 |A_{\parallel}^V|^2 \right. \\ &\quad \left. + 4\sqrt{2}\hat{m}_{K^*}\hat{m}_V(1 - \hat{m}_V^2 - \hat{m}_{K^*}^2) \right. \\ &\quad \left. \times |A_0^V| |A_{\parallel}^V| \cos(\delta_{\parallel}^V - \delta_0^V) \right)^{1/2}, \\ \sin(\delta_2^V - \delta_0^V) &= -\frac{\sqrt{2}}{|S_2^V| \lambda(1, \hat{m}_V^2, \hat{m}_{K^*}^2)} \\ &\quad \times (1 - \hat{m}_V^2 - \hat{m}_{K^*}^2) |A_{\parallel}^V| \sin(\delta_{\parallel}^V - \delta_0^V), \\ \cos(\delta_2^V - \delta_0^V) &= -\frac{\sqrt{2}}{|S_2^V| \lambda(1, \hat{m}_V^2, \hat{m}_{K^*}^2)} \\ &\quad \times \left( (1 - \hat{m}_V^2 - \hat{m}_{K^*}^2) |A_{\parallel}^V| \cos(\delta_{\parallel}^V - \delta_0^V) \right. \\ &\quad \left. + 2\sqrt{2}\hat{m}_V\hat{m}_{K^*} |A_0^V| \right), \\ \delta_1^V &\equiv \delta_{\parallel}^V \pmod{2\pi}, \quad \delta_3^V \equiv \delta_{\perp}^V \pmod{2\pi}. \end{aligned} \quad (\text{B13})$$

TABLE VI: Branching ratio [24], and decay amplitudes for  $B_d^0 \rightarrow K^{*0} \rho^0$  [25],  $B_d^0 \rightarrow K^{*0} \omega$  [25] and  $B_d^0 \rightarrow K^{*0} \phi$ ,  $B_d^0 \rightarrow K^{*0} J/\psi$ ,  $B_d^0 \rightarrow K^{*0} \psi(2S)$  [24].

$V$	$\rho^0$	$\omega$	$\phi$	$J/\psi$	$\psi(2S)$
$10^6 \text{BR}(B_d^0 \rightarrow K^{*0} V)$	3.4	2.0	9.8	1330	610
$ h_0^V ^2$	0.70	0.75	0.480	0.570	0.46
$ h_{\perp}^V ^2$	0.14	0.12	0.24	0.219	0.30
$\delta_0^V$ (rad)			2.82		
$\arg(h_{\parallel}^V/h_0^V)$ (rad)	1.17	1.79	2.40	-2.86	-2.8
$\arg(h_{\perp}^V/h_0^V)$ (rad)	1.17	1.82	2.39	3.01	2.8
$10^4  S_1^V $	1.17	0.81	2.66	33.64	28.86
$10^4  S_2^V $	2.65	1.67	5.20	42.49	52.65
$10^4  S_3^V $	2.31	1.64	5.28	115.28	153.00
$\delta_1^V - \delta_0^V$ (rad)	1.17	1.79	2.40	-2.86	-2.8
$\delta_2^V - \delta_0^V$ (rad)	-2.11	-1.53	-0.84	0.90	1.62
$\delta_3^V - \delta_0^V$ (rad)	1.17	1.82	2.39	3.01	2.8

- 
- [1] M. Antonelli, D.M. Asner, D. Bauer *et al.*, Phys. Rep. **494**, 197 (2010).
- [2] Y. Grossman and D. Pirjol, JHEP **06**, 029 (2000).
- [3] D. Melikhov, N. Nikitin, and S. Simula, Phys. Lett. B **442**, 381 (1998); F. Krüger, L.M. Sehgal, N. Sinha, and R. Sinha, Phys. Rev. D **61**, 114028 (2000); Phys. Rev. D **63**, 019901(E) (2001); C.S. Kim, Y.G. Kim, C.-D. Lu, and T. Morozumi, Phys. Rev. D **62**, 034013 (2000).
- [4] A. Ali, P. Ball, L.T. Handoko, and G. Hiller, Phys. Rev. D **61**, 074024 (2000); A. Ali, E. Lunghi, C. Greub, and G. Hiller, *ibid.* D **66**, 034002 (2002).
- [5] F. Krüger and J. Matias, Phys. Rev. D **71**, 094009 (2005).
- [6] C. Bobeth, G. Hiller, and G. Piranishvili, JHEP **07**, 106 (2008); U. Egede, T. Hurth, J. Matias, M. Ramon, and W. Reece, *ibid.* **11**, 032 (2008).
- [7] W. Altmannshofer, P. Ball, A. Bharucha, A.J. Buras, D.M. Straub, and M. Wick, JHEP **01**, 019 (2009).
- [8] U. Egede, T. Hurth, J. Matias, M. Ramon, and W. Reece, JHEP **10**, 056 (2010).
- [9] P. Ball and R. Zwicky, Phys. Rev. D **71**, 014029 (2005).
- [10] F. De Fazio, T. Feldmann, and T. Hurth, Nucl. Phys. B **733**, 1 (2006); Erratum-*ibid.* B **800**, 405 (2008); JHEP **0802**, 031 (2008).
- [11] B. Aubert *et al.*, (BABAR Collaboration), Phys. Rev. Lett. **102**, 091803 (2009).
- [12] J.-T. Wei *et al.*, (Belle Collaboration), Phys. Rev. Lett. **103**, 171801 (2009).
- [13] T. Aaltonen *et al.*, (CDF Collaboration), arXiv:1107.3753v1 [hep-ex]; T. Aaltonen *et al.*, (CDF Collaboration), arXiv:1108.0695v1 [hep-ex].
- [14] J. Lefrancois and M.H. Schune, LHCb-PUB-2009-008, 2009.
- [15] A.Yu. Korchin and V.A. Kovalchuk, Phys. Rev. D **82**, 034013 (2010).
- [16] Z. Ligeti and M.B. Wise, Phys. Rev. D **53**, 4937 (1996).
- [17] N.G. Deshpande, J. Trampetic, and K. Panose, Phys. Rev. D **39**, 1461 (1989); C.S. Lim, T. Morozumi, and A.I. Sanda, Phys. Lett. B **218**, 343 (1989); A. Ali, T. Mannel, and T. Morozumi, *ibid.*, B **273**, 505 (1991); F. Krüger and L.M. Sehgal, *ibid.*, B **380**, 199 (1996).
- [18] N. Cabibbo, Phys. Rev. Lett. **10**, 531 (1963); M. Kobayashi and T. Maskawa, Prog. Theor. Phys. **49**, 652 (1973).
- [19] R.P. Feynman, *Photon-hadron interactions*, W.A. Benjamin, Inc. Reading, Massachusetts, 1972.
- [20] F. Klingl, N. Kaiser, and W. Weise, Z. Phys. A **356**, 193 (1996).
- [21] H.B. O'Connell, B.C. Pearce, A.W. Thomas, and A.G. Williams, Prog. Nucl. Part. Phys. **39**, 201 (1997).
- [22] G. Ecker, J. Gasser, A. Pich, and E. de Rafael, Nucl. Phys. B **321**, 311, (1989).
- [23] S. Eidelman, S. Ivashyn, A. Korchin, G. Pancheri, and O. Shekhovtsova, Eur. Phys. J. C **69**, 103 (2010).
- [24] K. Nakamura *et al.* (Particle Data Group), J. Phys. G **37**, 075021 (2010).
- [25] C.H. Chen, arXiv:hep-ph/0601019v2.
- [26] M. Beneke, Th. Feldmann, and D. Seidel, Nucl. Phys. B **612**, 25 (2001).
- [27] B. Aubert *et al.*, (BABAR Collaboration), Phys. Rev. Lett. **98**, 051801 (2007).
- [28] G. Buchalla, A.J. Buras, and M.E. Lautenbacher, Rev. Mod. Phys. **68**, 1125 (1996).
- [29] N. Gray, D.J. Broadhurst, W. Grafe, and K. Schilcher, Z. Phys. C **48**, 673 (1990).
- [30] K.G. Chetyrkin and M. Steinhauser, Phys. Rev. Lett. **83**, 4001 (1999); K. Melnikov and T. van Ritbergen, Phys. Lett. B **482**, 99 (2000).
- [31] G. Valencia, Phys. Rev. D **39**, 3339 (1989).
- [32] This means the narrow-width approximation for the  $\bar{K}^{*0}$  propagator:  $(k^2 - m_{K^*}^2 + im_{K^*}\Gamma_{K^*})^{-1} \approx -i\pi\delta(k^2 - m_{K^*}^2)$ .
- [33] The term  $\propto q^\mu q^\nu/q^2$  in (37) does not contribute when contracted with the leptonic current